Infrared Physics & Technology 90 (2018) 95–100

Contents lists available at ScienceDirect

Infrared Physics & Technology

journal homepage: www.elsevier.com/locate/infrared

Regular article

Channeled polarimetric technique for the measurement of spectral dependence of linearly Stokes parameters

Naicheng Quan [a,*], Chunmin Zhang [b], Tingkui Mu [b], Qiwei Li [b]

[a] School of Materials Science and Engineering, Xi'an University of Technology, Xi'an 710048, China
[b] Institute of Space Optics, Xi'an Jiaotong University, Xi'an 710049, China

HIGHLIGHTS

- An achromatic quarter wave plate, a high order retarder and a fixed polarizer can acquire linearly wavelength-dependent Stokes parameters.
- Laboratory experiments demonstrated the spectropolarimetric capability of the method.
- The presented method can improve the resolution of the reconstructed linearly spectrally resolved Stokes parameters and suppress reconstruction errors caused by aliasing between the channels.

ARTICLE INFO

Article history:
Received 30 November 2017
Revised 28 February 2018
Accepted 1 March 2018
Available online 2 March 2018

Keywords:
Polarimetry
Channeled spectropolarimeter
Imaging spectropolarimeter

ABSTRACT

The principle and experimental demonstration of a method based on channeled polarimetric technique (CPT) to measure spectrally resolved linearly Stokes parameters (SRLS) is presented. By replacing front retarder with an achromatic quarter wave-plate of CPT, the linearly SRLS can be measured simultaneously. It also retains the advantages of static and compact of CPT. Besides, comparing with CPT, it can reduce the RMS error by nearly a factor of 2–5 for the individual linear Stokes parameters.

1. Introduction

Polarization information scattered or reflected from targets usually differs from that of background light and thus can offer targets' surface features, shape, shading, and roughness, while spectral information implies the targets' physical and chemical properties. Spectropolarimeter can acquire the spectral dependence of state of polarization (SOP) and improves the ability to effectively recognize the target with preferable accuracy [1–5].

Since conventional spectropolarimeters usually install polarization switching elements and microretarder or micropolarizer arrays in spectrometers, the sensors generally suffer from vibration, electrical noise, heat generation, and alignment difficulty [7]. CPT is first implemented by Oka and Kato, and can acquire all the spectrally resolved Stokes parameters at once without movable polarization components or micro-components [8]. Based on this concept, the CPT is incorporated into different imaging Fourier transform spectrometer to form Fourier transform channeled imaging spectropolarimeter (FTCISP) that has unique benefits due to the throughput (Jacquinot) and multiplex (Fellgett) advantages [9–16]. Recent progresses in imaging schemes arouse numerous potential applications of FTCISP in fields of target recognition [17,18], biomedical and material diagnosis [19,20], and atmospheric remote sensing [21]. Such sensor adds two thick retarders and an analyzer before imaging spectrometers or interferometers and yields direct access to the spectral carrier frequencies containing the spectrally resolved Stokes parameters. Since the interferogram recorded by the sensor usually contains seven interference channels, the spectral resolution of each spectral Stokes parameters is much lower than that of the interferometer. Besides, there is aliasing among the fringe patterns of different Stokes parameters, when a narrowband spectrum is measured by such sensor. An artifact reduction technique (ART) was addressed to eliminate the dominant aliasing between the interference channels. Since ART is performed by combining double measurements with orienting the analyzer in two orthogonal directions, a longer scanning time is needed, which makes the system more susceptible to temporal misregistration [13]. Recently, several improving aperture/amplitude division methods were proposed to modulate the Stokes

* Corresponding author.
E-mail address: quanncx@hotmail.com (N. Quan).

https://doi.org/10.1016/j.infrared.2018.03.002
1350-4495/

parameters into imaging spectrometer to overcome the general drawbacks of the FTCISP [12,17,18]. However, differences in the distortion, focal length, and transmission coefficient of the optics necessitate sophisticated image registration algorithms. It is generally known that the measurement of S_3 is not necessary in most passive imaging scenarios that the obtaining linearly spectrally resolved Stokes parameters would satisfy several applications [6].

In this paper, we presented a method based on channeled polarimetric technique to measure spectrally resolved linearly Stokes parameters (namely, full linearly channeled polarimetric technique, FLCPT) that can increase spectral resolution of each measured Stokes parameter and restrain measurement error caused by aliasing between the channels. We describe the principle of the method in Section 2. The performance of the proposed method and conventional channeled polarimetric technique is compared through an experiment in Section 3, while our conclusion is contained in Section 4.

2. Principle of FLCPT

Optical schematic of the FLCPT is depicted in Fig. 1. The Stokes vector $S(\sigma)$ emitting from the target passes through achromatic quarter wave-plate AQWP, high-order retarder R and a linear analyzer, LA. The spectrum of the exiting light is then recorded by the spectrometer. The fast axis of AQWP is aligned with the transmission axis of LA, and R is oriented with its fast axis at 45° to the transmission axis of LA.

By using the Mueller calculus, the Stokes vector of the emergent light from analyzer LA can be described as [8,14]

$$\mathbf{S_{out}} = \mathbf{M_{LA}}\mathbf{M_R}\mathbf{M_{AQWP}}\mathbf{S_{in}} \tag{1}$$

where $\mathbf{M_{AQWP}}$, $\mathbf{M_R}$ and $\mathbf{M_{LA}}$ are the Muller matrices of the achromatic quarter wave plate AQWP, retarder R and the analyzer P_2, respectively. $\mathbf{S_{in}}$ is the spectrally resolved Stokes vector of the incident light and expressed by

$$S(\sigma) = \begin{bmatrix} S_0(\sigma) \\ S_1(\sigma) \\ S_2(\sigma) \\ S_3(\sigma) \end{bmatrix} = \begin{bmatrix} I_{0^\circ}(\sigma) + I_{90^\circ}(\sigma) \\ I_{0^\circ}(\sigma) - I_{90^\circ}(\sigma) \\ I_{45^\circ}(\sigma) + I_{-45^\circ}(\sigma) \\ I_R(\sigma) - I_L(\sigma) \end{bmatrix} \tag{2}$$

where σ is spectral variable, $S_0(\sigma)$ is the total intensity of the light, while $S_1(\sigma)$ denotes the part of 0° linear polarized light over 90°, $S_2(\sigma)$ for +45° over −45°, and $S_3(\sigma)$ for right circular over left circular.

The spectrometer responds to radiation intensity instead of polarization state, so only the first parameter of $\mathbf{S_{out}}$ can be measured. The recorded signal is varied with wavenumber and can be expressed as

$$S_0^{out}(\sigma) = \frac{1}{2}[S_0(\sigma) + S_1(\sigma)cos\varphi_R(\sigma) + sin\varphi_R(\sigma)S_2(\sigma)] \tag{3}$$

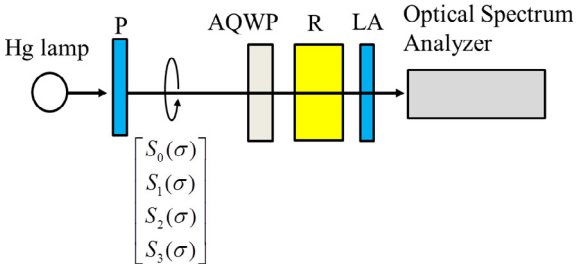

Fig. 1. Optical schematic of FLCPT.

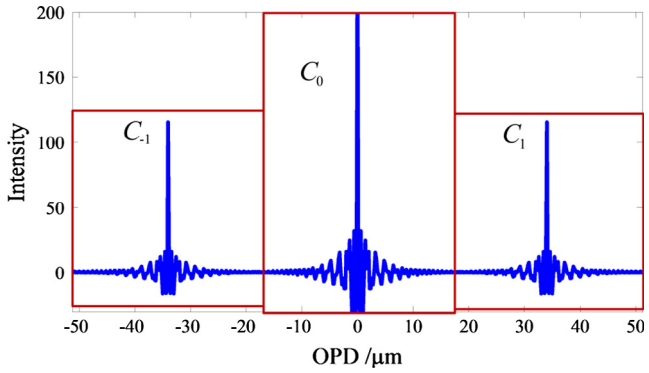

Fig. 2. Simulated interferogram for a 0° linear incident polarization state.

The phase term is presented as$\varphi_R(\sigma) = 2\pi\sigma B(\sigma)D$, where $B(\sigma)$ and D is birefringence of the crystal and thickness of the retarder R, respectively. It should be noted that such a cosinusoidally modulated spectrum is the channeled spectrum that is frequently used in the field of frequency-domain interferometry. Expanding Eq. (3) yields three frequency channels that contain the polarimetric information

$$S_0^{out}(\sigma) = \frac{1}{2}S_0(\sigma) + \frac{S_1(\sigma) - iS_2(\sigma)}{4}e^{i\varphi} + \frac{S_1(\sigma) + iS_2(\sigma)}{4}e^{-i\varphi} \tag{4}$$

The inverse Fourier transformation of $S_0^{out}(\sigma)$ gives an interferogram with the intensity varied with optical path difference:

$$C(z) = \frac{1}{2}C_0(z) + \frac{1}{4}C_1(z - L_2) + \frac{1}{4}C_1^*(-z - L_2) \tag{5}$$

where z and L_2 denotes the optical path difference (*OPD*) produce by the spectrometer and the retarder R, respectively. The three components included in $C(z)$, centered at $z = 0$ and $\pm L_2$, are separated from one another over the *OPD* axis if the retarder thickness D is properly selected. These separated channels can be seen from a simulated interferogram shown in Fig. 2, where the input radiation is a 0° linear incident polarization state and a broad band source.

By filtering the desired channels C_0 and C_{-1} (fringe patterns in the left two red boxes shown in Fig. 2) and taking Fourier transform, the linearly spectrally-dependent Stokes parameters can be reconstructed:

$$S_0(\sigma) = \Im\{C_0\} \tag{6}$$

$$S_1 = \text{real}[2\Im\{C_1\}e^{i\varphi}] \tag{7}$$

$$S_2 = \text{imag}[2\Im\{C_1\}e^{i\varphi}] \tag{8}$$

where real[ ] and imag[ ] denotes taking the real part and imaginary part of an imaginary parameter. In Eqs. (6)–(8), $S_0(\sigma)$ can be demodulated directly, the phase factor φ modulated $S_1(\sigma)$ and $S_2(\sigma)$ can be calibrated by using a reference beam [8,13,14].

3. Experiment and discussion

We carried out an experiment to demonstrate the validity of our method. Polychromatic light from an Hg lamp is transmitted by a polarizer (P) located in front of the AQWP to create a controlled SOP. The polarizer and the analyzer are α-barium borate (α-BBO) Glan-Taylor prisms (extinction ratio $\geq 10^5$) from Union Optic, Inc. AQWP is the product AQWP05M-600 supplied by Thorlabs, Inc with flat retardance of 90° over 400–800 nm. The quartz prism with thickness of 9 mm fabricated by Keelaser, Inc is used for the retarder. Spectrum $S_0^{out}(\sigma)$of the light transmitted by LA is

taken with an optical spectrum analyzer (AvaSpec-ULS2048) over the wavenumber range from σ = 16207.46–20833.33 cm^{-1} (wavelength λ = 480–617 nm). The wavelength resolution of the optical spectrum analyzer is 1 nm, and its sampling number is 2048. The azimuth of the polarizer relative transmission axis of LA is set to be 60° and 45° to generate two different linearly SOP ($S_{in60°}$ = S_0[1–0.5 0.866 0], $S_{in45°}$ = S_0[1 0 1 0]), respectively.

The channeled spectrum $S_0^{out}(\sigma)$modulated with the wavenumber dependence of the phase retardation is shown in Fig. 3. The magnitude of the inverse Fourier transformation of $S_0^{out}(\sigma)$is shown Fig. 4. It can be seen that the three components included in $C(z)$ are successfully separated from one another over the *OPD* axis. The linearly wavenumber dependent Stokes parameters can then be calculated from $C(z)$ by using Eqs. (6)–(8).

Note that the Stokes parameter $S_0(\sigma)$is the intensity spectrum of the incident light (independent of the polarization state). Fig. 5 depicts the reconstructed spectrum, together with the spectrum recorded by Analytical Spectral Devices, Inc. (ASD) spectroradiometer. The normalized values $S_1(\sigma)/S_0(\sigma)$and $S_2(\sigma)/S_0(\sigma)$are shown in Fig. 6. Compare with the theoretical values, the experimental results exhibit favorable accordance, and the feasibility of the present method is validated.

In order to further demonstrate the advantage of the presented method, the same input signal was measured by the conventional channeled polarimetric technique (CCPT). The AQWP in the experimental setup illustrated in Fig. 1 is replaced by a quartz retarder with thickness of 4.5 mm. The magnitude of the inverse Fourier transformation of $S_0^{out}(\sigma)$included seven components separated

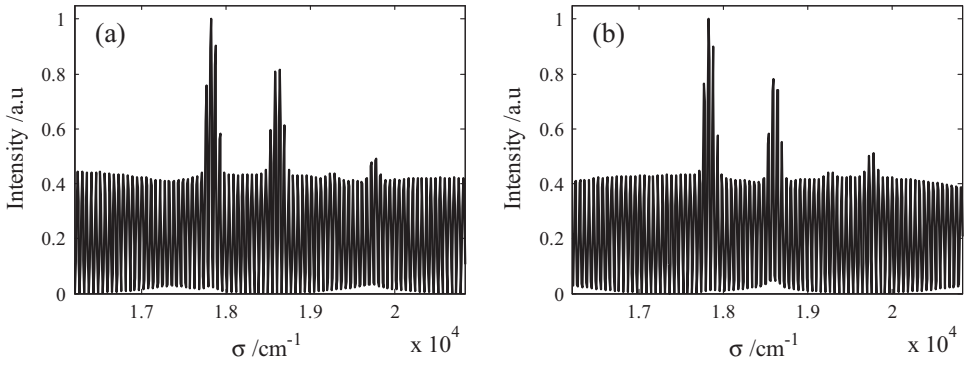

Fig. 3. Measured channeled spectrum $S_0^{out}(\sigma)$corresponds to (a) 60° linearly polarized light (b) 45° linearly polarized light.

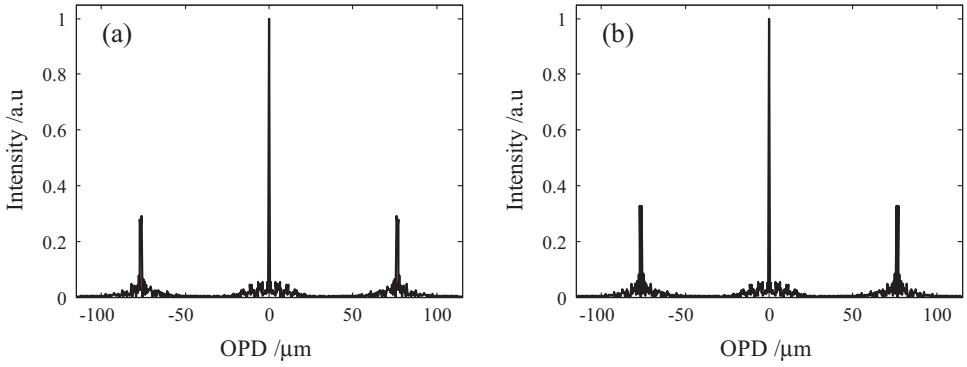

Fig. 4. The magnitude of the inverse Fourier transformation of $S_0^{out}(\sigma)$corresponds to (a) 60° linearly polarized light (b) 45° linearly polarized light.

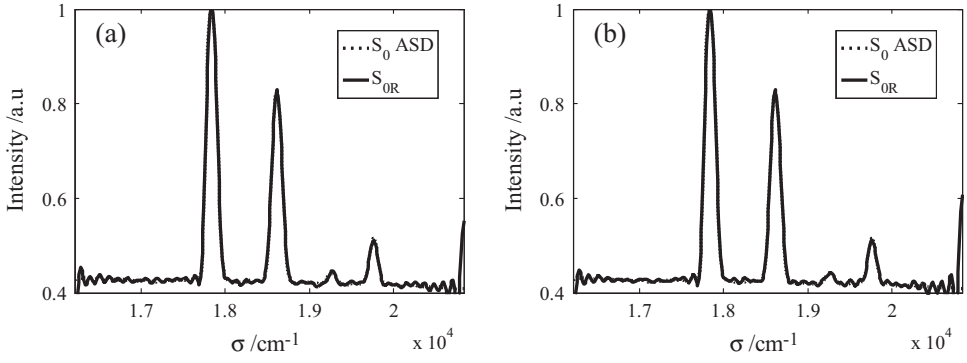

Fig. 5. The Demodulated spectrum $S_0(\sigma)$corresponds to (a) 60° linearly polarized light (b) 45° linearly polarized light.

from one another over the *OPD* axis, which is shown in Fig. 7. According to the literature [8], the linearly spectrally resolved Stokes parameters can be reconstructed by filtering three desired channels in Fig. 8, and the results are shown in Figs. 8 and 9.

Compare Fig. 5 with Fig. 8, $S_0(\sigma)$reconstructed by FLCPT fully displays the sharp lines located at the wavenumber of 17,820 cm^{-1} and 18,600 cm^{-1} in the incident spectrum. Consequently, previously unresolvable spectral features are now resolvable via the FLCPT. The normalized spectrally resolved Stokes parameters shown in Figs. 6 and 9 include the reconstructed error caused by crosstalk between the channels; it also exists in the reconstructed$S_0(\sigma)$. Tables 1 and 2 display the RMS error of the individual reconstructed linearly spectrally resolved Stokes parameters over the 16207.46–20833.33 cm^{-1} spectral band, respectively. It can be seen that the method presented in this paper reduces the RMS error by nearly a factor of 2–5 for the individual linear Stokes parameters. This is because the reduction in the number of superimposed interference fringes in FLCPT makes a weakened aliasing and a raised OPD of the filtered patterns.

The major advantage of FLCPT is that it can improve the resolution of the reconstructed linearly spectrally resolved Stokes parameters and suppress reconstruction errors caused by aliasing between the channels. It also has the advantage that there is no mechanically movable component for polarization control or active components for polarization modulation in the configuration to measure the spectrally resolved Stokes parameters. The concept of the present method is based primarily on the fact that the phase retardation of the AQWP is a constant value of 90° for

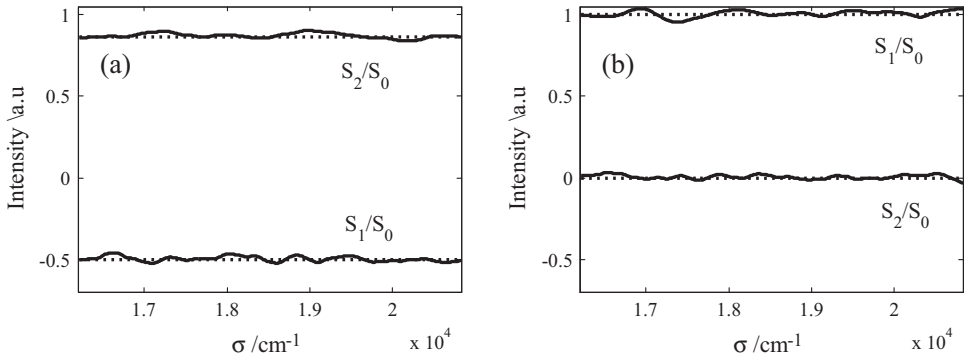

Fig. 6. The normalized linearly spectrally resolved Stokes parameters corresponds to (a) 60° linearly polarized light (b) 45° linearly polarized light.

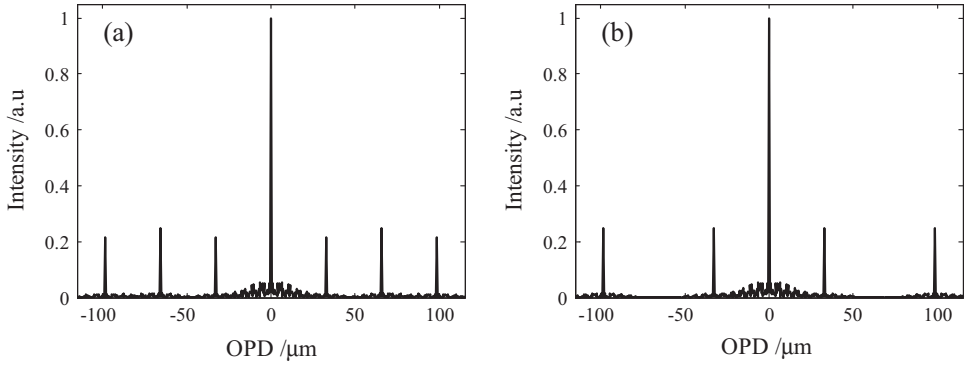

Fig. 7. The magnitude of the inverse Fourier transformation of $S_0^{out}(\sigma)$obtained by CCPT corresponds to (a) 60° linearly polarized light (b) 45° linearly polarized light.

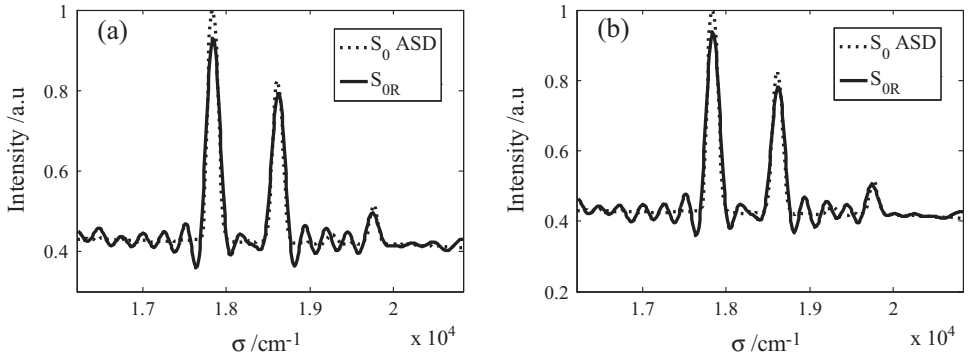

Fig. 8. The spectrum $S_0(\sigma)$reconstructed by CCPT corresponds to (a) 60° linearly polarized light (b) 45° linearly polarized light.

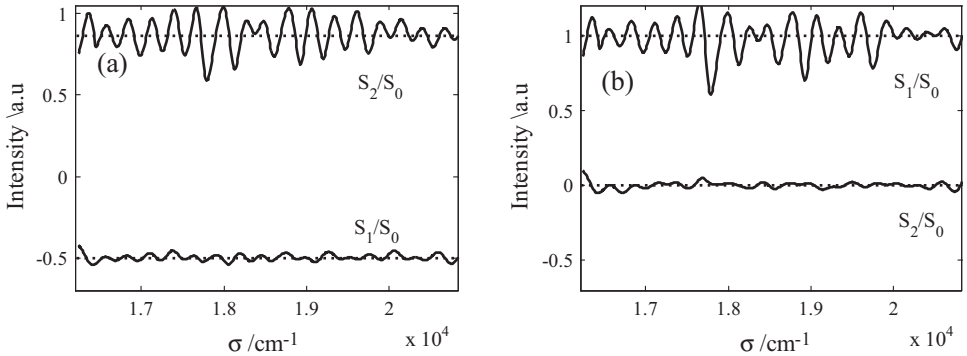

Fig. 9. The normalized linearly spectrally resolved Stokes parameters reconstructed by FLCPT corresponds to (a) 60° linearly polarized light (b) 45° linearly polarized light.

Table 1
RMS error across 16207.46–20833.33 cm^{-1} for 60° polarized light.

60° polarized light	$S_0(\sigma)$	$S_1(\sigma)$	$S_2(\sigma)$
CCPT reconstruction	2.53%	4.82%	11.75%
FLCPT reconstruction	1.52%	2.14%	4.32%
Difference	1.01%	2.68%	7.43%

Table 2
RMS error across 16207.46–20833.33 cm^{-1} for 45° polarized light.

45° polarized light	$S_0(\sigma)$	$S_1(\sigma)$	$S_2(\sigma)$
CCPT reconstruction	2.48%	12.36%	4.39%
FLCPT reconstruction	1.49%	2.83%	2.57%
Difference	0.99%	9.53%	1.82%

different wavenumbers. This makes the number of channels be dropped from 7 to 3 comparing with the CCPT, which leads to an increasing interval between the channels. That is why the present method can overcome the two drawbacks of CCPT.

4. Conclusion

In this paper, we presented a method to acquire the linearly wavelength-dependent Stokes parameters based on the channeled polarimetric technique. By replacing front retarder with an achromatic quarter wave-plate, linearly wavelength-dependent Stokes parameters can be measured simultaneously. The achromatic quarter wave-plate produced a constant retardation of 90° which makes the number of channels in the conventional channeled polarimetric technique dropped from 7 to 3 and interval between the channels increased obviously. Laboratory experiments of mercury lamp lights illuminating a broadband polarizer demonstrated the spectropolarimetric capability of the method. Compared with the conventional channeled polarimetric technique, the presented method can improve the resolution of the reconstructed linearly spectrally resolved Stokes parameters and suppress reconstruction errors caused by aliasing between the channels. Further work will install the method to our static interference imaging spectrometer based on Savart polariscope to form a static hyperspectral imaging polarimeter for full linear Stokes parameters.

Conflict of interest

None declared.

Acknowledgements

The authors thank the anonymous reviewers for their helpful comments and constructive suggestions. The work was supported by the scientific research support program for new teacher of Xi'an University of technology (101-256081706) and National Natural Science Foundation (61275184) of China.

Appendix A. Supplementary material

Supplementary data associated with this article can be found, in the online version, at https://doi.org/10.1016/j.infrared.2018.03.002.

References

[1] D.J. Diner, R.A. Chipman, N. Beaudry, B. Cairns, L.D. Food, S.A. Macenka, T.J. Cunningham, S. Seshadri, C. Keller, An integrated multiangle, multispectral, and polarimetric imaging concept for aerosol remote sensing from space, Proc. SPIE 5659 (2005) 88–96.
[2] F. Snik, T. Karalidi, C.U. Keller, Spectral modulation for full linear polarimetry, Appl. Opt. 48 (2009) 1337–1346.
[3] W. Groner, J.W. Winkelman, A.G. Harris, C. Ince, G.J. Bouma, K. Messmer, R.G. Nadeau, Orthogonal polarization spectral imaging: A new method for study of the microcirculation, Nat. Med. 5 (1999) 1209–1212.
[4] T.G. Moran, J.M. Davila, Three-dimensional polarimetric imaging of coronal mass ejections, Science 305 (2004) 66–70.
[5] R.S. Gurjar, V. Backman, L.T. Perelman, I. Georgakoudi, K. Badizadegan, I. Itzkan, R.R. Dasari, M.S. Feld, Imaging human epithelial properties with polarized light-scattering spectroscopy, Nat. Med. 7 (2001) 1245–1248.
[6] J.S. Tyo, D.L. Goldstein, D.B. Chenault, J.A. Shaw, Review of passive imaging polarimetry for remote sensing applications, Appl. Opt. 45 (2006) 5453–5469.
[7] J. Li, J.P. Zhu, H.Y. Wu, Compact static Fourier transform imaging spectropolarimeter based on channeled polarimetry, Opt. Lett. 35 (2010) 3784–3786.
[8] K. Oka, T. Kato, Spectroscopic polarimetry with a channeled spectrum, Opt. Lett. 24 (1999) 1475–1477.
[9] J.S. Tyo, T.S. Turner, Variable-retardance, Fourier-transform imaging spectropolarimeters for visible spectrum remote sensing, Appl. Opt. 40 (2001) 1450–1458.
[10] S.H. Jones, F.J. Iannarilli, P.L. Kebabian, Realization of quantitative-grade fieldable snapshot imaging spectropolarimeter, Opt. Express 12 (2004) 6559–6573.
[11] R.W. Aumiller, C. Vandervlugt, E.L. Dereniak, R. Sampson, R.W. McMillan, Snapshot imaging spectropolarimetry in the visible and infrared, Proc. SPIE 6972 (2008) D1–D9.
[12] X. Meng, J. Li, D. Liu, R. Zhu, Fourier transform imaging spectropolarimeter using simultaneous polarization modulation, Opt. Lett. 38 (2013) 778–780.
[13] J.C. Jones, M.W. Kudenov, M.G. Stapelbroek, E.L. Dereniak, Infrared hyperspectral imaging polarimeter using birefringent prisms, Appl. Opt. 50 (2011) 1170–1185.
[14] M.W. Kudenov, N.A. Hagen, E.L. Dereniak, G.R. Gerhart, Fourier transform channeled spectropolarimetry in the MWIR, Opt. Express 15 (2007) 12792–12805.
[15] J. Li, B. Gao, C. Qi, J.P. Zhu, X. Hou, Tests of a compact static Fourier-transform imaging spectropolarimeter, Opt. Express 22 (2014) 13014–13021.

[16] C. Zhang, Q. Li, T. Yan, T. Mu, Y. Wei, High throughput static channeled interference imaging spectropolarimeter based on a Savart polariscope, Opt. Express 24 (2016) 23314–23332.
[17] T. Mu, C. Zhang, C. Jia, W. Ren, Static hyperspectral imaging polarimeter for full linear Stokes parameters, Opt. Express 20 (2012) 18194–18201.
[18] T. Mu, C. Zhang, C. Jia, W. Ren, Static polarization-difference interference imaging spectrometer, Opt. Lett. 37 (2012) 3507–3509.
[19] S. Guyot, M. Anastasiadou, E. Deléchelle, A.D. Martino, Registration scheme suitable to Mueller matrix imaging for biomedical applications, Opt. Express 15 (2007) 7393–7400.
[20] C. Zhang, B. Xiangli, B. Zhao, X. Yuan, A static polarization imaging spectrometer based on a Savart polariscope, Opt. Commun. 203 (2002) 21–26.
[21] T. Mu, C. Zhang, B. Zhao, Principle and analysis of a polarization imaging spectrometer, Appl. Opt. 48 (2009) 2333–2339.